

polymer papers

The structure of copoly(4-hydroxybenzoic acid/2-hydroxy-6-naphthoic acid):

2. An atomic model for the copolyester chain*

Robin A. Chivers, John Blackwell and Genaro A. Gutierrez

Department of Macromolecular Science, Case Western Reserve University, Cleveland, Ohio 44106, USA

(Received 8 June 1983)

X-ray fibre diagrams of fibres drawn from the (liquid crystalline) melts of copoly(4-hydroxybenzoic acid/2-hydroxy-6-naphthoic acid) show meridional maxima that are aperiodic. The positions of these maxima are reproduced in calculations of the meridional intensities for completely random copolymer sequences in which the monomers are approximated to points separated by the appropriate monomer lengths. These calculations have now been extended to consider an atomic model for the chains. Comparison of the calculated meridional transforms with diffractometer scans for five monomer ratios shows good agreement, not only for the positions but also for the relative intensities of the observed and calculated maxima. The linewidth of the maximum at $d \approx 2.1$ Å depends on the chain length used for the calculations and presents a method for determination of the persistence length of the extended chain conformation.

Keywords X-ray diffraction; liquid crystalline polymers; copolyesters; thermotropic polymers; structure determination

INTRODUCTION

Poly(4-hydroxybenzoic acid) and other similar aromatic homopolyesters are crystalline, infusible, largely intractable solids. However, many copolyesters prepared from their monomers form liquid crystalline melts and can be processed as high-strength fibres and novel self-reinforced moulded plastics. The chemical structures and properties of these thermotropic copolyesters have been reviewed by Jin *et al.*¹

In this paper we describe X-ray analyses of the structure of one of these systems, the wholly aromatic copolyester prepared from 4-hydroxybenzoic acid (HBA) and 2-hydroxy-6-naphthoic acid (HNA). The X-ray diffraction patterns of melt-spun fibres of this copolyester show a high degree of molecular orientation parallel to the fibre axis, and there is also some ordered lateral packing. A striking feature of the X-ray data is that the meridional maxima are *aperiodic*, i.e. they are not orders of a simple repeat, and their positions vary with the monomer ratio. We have shown that the positions of these maxima are reproduced in calculations of the Fourier transforms of chains of completely random sequence in which the monomers are approximated by points separated by the appropriate monomer lengths². Previous work on the analogous copolyesters prepared from HBA, 2,6-dihydroxynaphthalene and terephthalic acid showed that in this system the aperiodic meridional maxima could also be reproduced by a completely random sequence modelled by point residues³.

The above calculations gave good agreement for the positions of the maxima, but the intensities could not be compared because the intra-residue interferences are not considered when the residues are approximated to points. In addition the calculations used a random number generator to set up the monomer sequences, and this leads to statistical variations in the results, due to the limited sample size that can be considered without use of excessive computer time. Methods to overcome these difficulties have been described by Blackwell *et al.*⁴. The procedure is to calculate the Fourier transform of the autocorrelation function of the chain, which for a point residue approximation is given by:

$$I(Z) = \sum_i Q(z_i) \exp(2\pi i Z z_i) \quad (1)$$

$Q(z_i)$ is the autocorrelation function of the chain of point monomers, and is the probability of neighbour residues separated by z_i . Z is the reciprocal space coordinate along the axis corresponding to the meridian of the X-ray pattern. Conversion to an atomic model is achieved by multiplying $Q(z_i)$ by the Fourier transform of the cross-convolution function $F_{AB}(Z)$ for the appropriate pair of neighbouring monomers A and B :

$$I(Z) = \sum_i \sum_A \sum_B Q(z_i) F_{AB}(Z) \exp(2\pi i Z z_i) \quad (2)$$

where

$$F_{AB}(Z) = \sum_j \sum_k f_{A,j} f_{B,k} \exp[2\pi i Z (z_{B,k} - z_{A,j})] \quad (3)$$

The subscript pairs A,j and B,k designate the j th atom in residue A and the k th atom in residue B . In equation (3) residues A and B have the same origin. In the present

* Paper 1 of this series is Gutierrez *et al.*²

example, $Q(z)$ is effectively divided into four components corresponding to the contributions of HBA...HBA, HBA...HNA, HNA...HBA and HNA...HNA neighbour relationships.

This paper describes the calculation of the meridional transforms for both point and atomic residue models for HBA/HNA copolymer chains, and compares the results with observed meridional diffractometer scans for five monomer ratios.

EXPERIMENTAL

Specimens of the copolymers were prepared at Celanese Research Company following the method described by Calundann⁵. Five HBA/HNA monomer ratios were examined: 25/75, 30/70, 50/50, 58/42 and 75/25. Fibres were drawn from molten chips and X-ray data were recorded using Ni-filtered $\text{Cu K}\alpha$ radiation, both on Kodak no-screen film using a Searle toroidal focusing camera, and also as a $\theta/2\theta$ meridional scan on a Philips D-76 diffractometer.

Atomic coordinates for the HBA and HNA residues were derived using standard bond lengths and angles. The aromatic and carboxyl groups were assumed to be rigid and the phenyl-carboxyl torsion angle was set at 30° . The ester oxygen-ester oxygen vector was assumed to be parallel to the chain axis, giving lengths of 6.35 Å and 8.37 Å for the HBA and HNA residues respectively. Atomic coordinates for the two residues are given in Table 1, and their structures are shown in Figure 1a. Figure 1b shows a typical short random sequence for the polymer chain. The meridional intensity, $I(Z)$, depends on the z -axis projection of the chain, which is approximately independent of conformation because the residue linkages are nearly parallel to the chain axis.

The theoretical meridional intensity was calculated using both the point and atomic models (equations (1)–(3)) for all five HBA/HNA ratios. The calculated data were

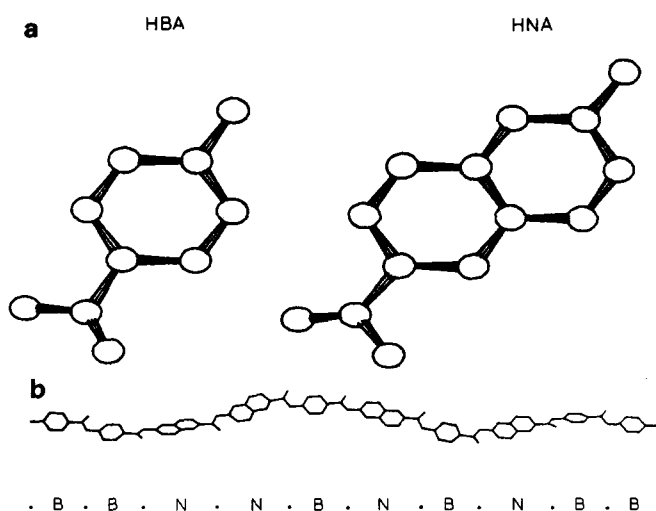


Figure 1 (a) Atomic models for the HBA and HNA residues. (b) Model for a typical short random copolymer sequence (10 residues) with its axial projection and the point residue approximation. It can be seen that the ester oxygen-ester oxygen vectors are approximately parallel to the chain axis

corrected for the Lorentz and polarization (L_p) effects to permit direct comparison with the observed intensities. The autocorrelation function $Q(z)$ was calculated as the neighbour probability distribution for completely random chains at the selected monomer ratios. The curves shown in Figure 2 were obtained for a normal distribution of chain lengths about an average of 10 residues. Use of this distribution function smooths the subsidiary maxima that occur close to the peaks at the origin and at $d \approx 2.1$ Å. The curves in Figure 4a are for monodisperse chains of 6, 8, 10 and 15 residues, for comparison of the effect of chain length on the line profiles.

RESULTS

Schematics of the X-ray fibre diagrams for the 30/70, 58/42 and 75/25 copolymers are shown in Figure 2. The original X-ray patterns were published in ref. 2. Meridional diffractometer scans for all five compositions are shown in Figures 3a–e and the positions of the observed meridional maxima are given in Table 2.

The film X-ray data show that there is a high degree of axial orientation of the molecules, as judged by the relatively short arcs of the intensity maxima. For the present, we shall concentrate on the meridional data; interpretation of the equatorial and off-equatorial scattering will be the subject of a future paper.

Figures 3a–e also include the calculated axial intensity distribution obtained from both the point and atomic models of chains of average length 10 residues.

It can be seen that a very good agreement is obtained in all cases for the number and positions of the observed and calculated maxima. In previous papers^{2,4}, we calculated data for a range of HBA/HNA monomer ratios from 0/100 to 100/0 in 10 percentage point increments. This showed clearly the steady shift in peak positions, and the change from three peaks in the HBA-rich compounds to four as the HNA content increased above 50%. The peak at $d \approx 2.1$ Å shows little change across the entire range, and this is due to the fact that the HBA and HNA residue lengths are fortuitously in the approximate ratio of 3:4.

Table 1 Atomic coordinates

HBA	x	y	z
Ester oxygen	0.00	0.00	0.00
Carbonyl carbon	0.00	-1.14	0.77
Carbonyl oxygen	-0.02	-2.24	0.31
Phenyl carbon 1	0.03	-0.80	2.22
Phenyl carbon 2	0.63	0.36	2.72
Phenyl carbon 3	-0.59	-1.70	3.09
Phenyl carbon 4	0.62	0.62	4.09
Phenyl carbon 5	-0.61	-1.44	4.47
Phenyl carbon 6	0.00	-0.28	4.97
Ester oxygen	0.00	0.00	6.35
HNA	x	y	z
Ester oxygen	0.00	0.00	0.00
Carbonyl carbon	0.00	-1.25	0.56
Carbonyl oxygen	0.06	-2.25	-0.09
Naphthyl carbon 1	-0.09	-1.17	2.04
Naphthyl carbon 2	-0.72	-2.23	2.69
Naphthyl carbon 3	0.43	-0.10	2.77
Naphthyl carbon 4	-0.84	-2.23	4.09
Naphthyl carbon 5	0.32	-0.09	4.17
Naphthyl carbon 6	-0.32	-1.15	4.83
Naphthyl carbon 7	0.83	0.98	4.91
Naphthyl carbon 8	-0.44	-1.15	6.22
Naphthyl carbon 9	0.72	0.99	6.30
Naphthyl carbon 10	0.08	-0.07	6.96
Ester oxygen	0.00	0.00	8.37

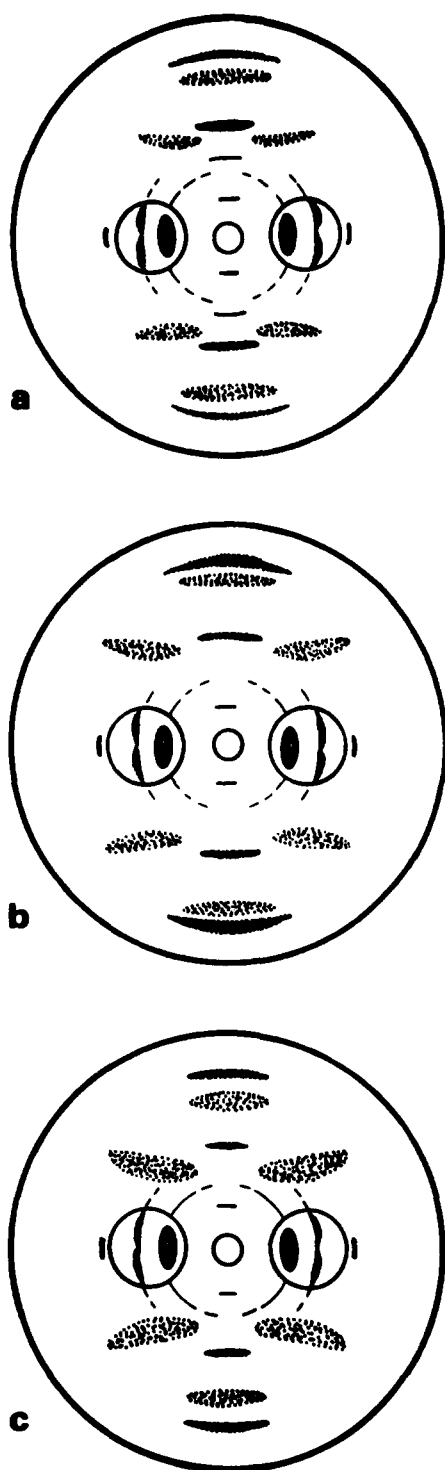


Figure 2 Schematics of the X-ray fibre diagrams of HBA/HNA copolyester for three monomer ratios: (a) 30/70; (b) 58/42; (c) 75/25

The present results cover a large part of this range and show precisely this predicted variation. Comparisons of the observed intensities and those calculated for the atomic models also show good agreement: the only discrepancy is for the peak at $d = 7-8 \text{ \AA}$, which is generally weaker than observed. These intensity data are discussed further below.

Figure 4a shows data for just one monomer ratio, 58/42, calculated using the atomic model for four different chain lengths from 6 residues up to 15. All have the same three peaks, although for the shortest chains, that at $7-8 \text{ \AA}$ is

distorted. Aside from this and the subsidiary maxima, which are a consequence of using a single chain length rather than the more reasonable distribution of lengths, the major difference occurs in the width of the maximum at 2.10 \AA . The calculated curves have been normalized to the same scattering intensity at $Z = 0$ in order to show this more clearly. The halfwidths of this peak are 2.0° for 6 residues, 1.5° for 8 residues, 1.2° for 10 residues and 0.8° for 15 residues. The observed halfwidth of the same peak in the diffractometer scan of the 58/42 copolymer is 1.3° , which is reduced to 1.1° when corrected for instrumental broadening. This diffractometer scan is shown in Figure 4b on the same scale as Figure 4a. These data suggest that approximately 11 residues is a reasonable value for the average chain persistence length for this composition. Comparison of the observed data for the five compositions shows the interesting effect that the linewidth at $d \approx 2.1 \text{ \AA}$ increases with increasing HBA content: the corrected linewidths are 1.4° , 1.3° , 1.1° , 1.1° and 1.0° for the 25/75, 30/70, 50/50, 58/42 and 75/25 monomer ratios. The relationship of chain length to (theoretical) linewidth is approximately the same for all five compositions and hence the persistence length appears to increase from ~ 9 to ~ 13 with increasing HBA content across the series. In addition, Figure 4a shows that, once the chain is greater than about eight residues, the profiles of the other maxima are almost independent of the length in the range considered.

DISCUSSION

It can be seen from Figure 3 and Table 2 that the random copolymer models lead to good agreement in the peak positions between the observed and calculated data. Calculations for the point model using the correlation function are similar to those reported previously for models set up using a random number generator, but are not noisy or subject to statistical fluctuations due to use of a limited sample. In addition, the subsidiary maxima have been smoothed away by use of a distribution of chain lengths about a selected average value.

Good agreement between the observed and calculated intensities cannot be expected for the point model because the effects of intra-residue interferences have not been considered. Examination of the L_p corrected data for the point models in Figure 3 shows that the 2.1 \AA maxima are generally much weaker than observed while the maxima calculated in the $7-8 \text{ \AA}$ range are much more intense. Conversion to the atomic model significantly improves the agreement. In particular the 2.1 \AA peak is now much more intense and is by far the strongest intensity, as it is in the observed data. Agreement is reasonable for the other peaks, except that the innermost peak at $7-8 \text{ \AA}$ is now weaker than observed.

The reason for these intensity changes can be seen in Figure 5 which shows the Fourier transforms of the self-convolutions, $F_{AA}(Z)$, for the monomers HBA and HNA. The intensity calculated via equation (2) is a weighted product of these (and also the cross-terms, $F_{AB}(Z)$) and the transform of the point model. Thus, features common to these $F_{AA}(Z)$ functions will modulate the transform of the point model, mainly affecting the intensities of the peaks. It can be seen that the monomer transforms have maxima at values of Z corresponding approximately to the monomer lengths, and then fluctuate slowly up to a maximum at $\sim 2 \text{ \AA}$. Thus, in the atomic model, the peak

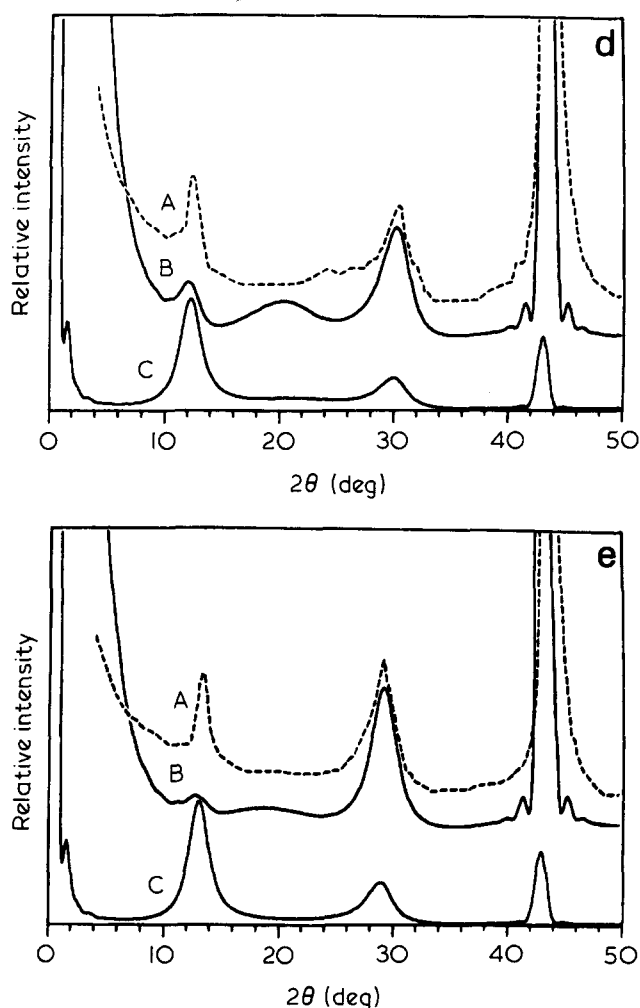
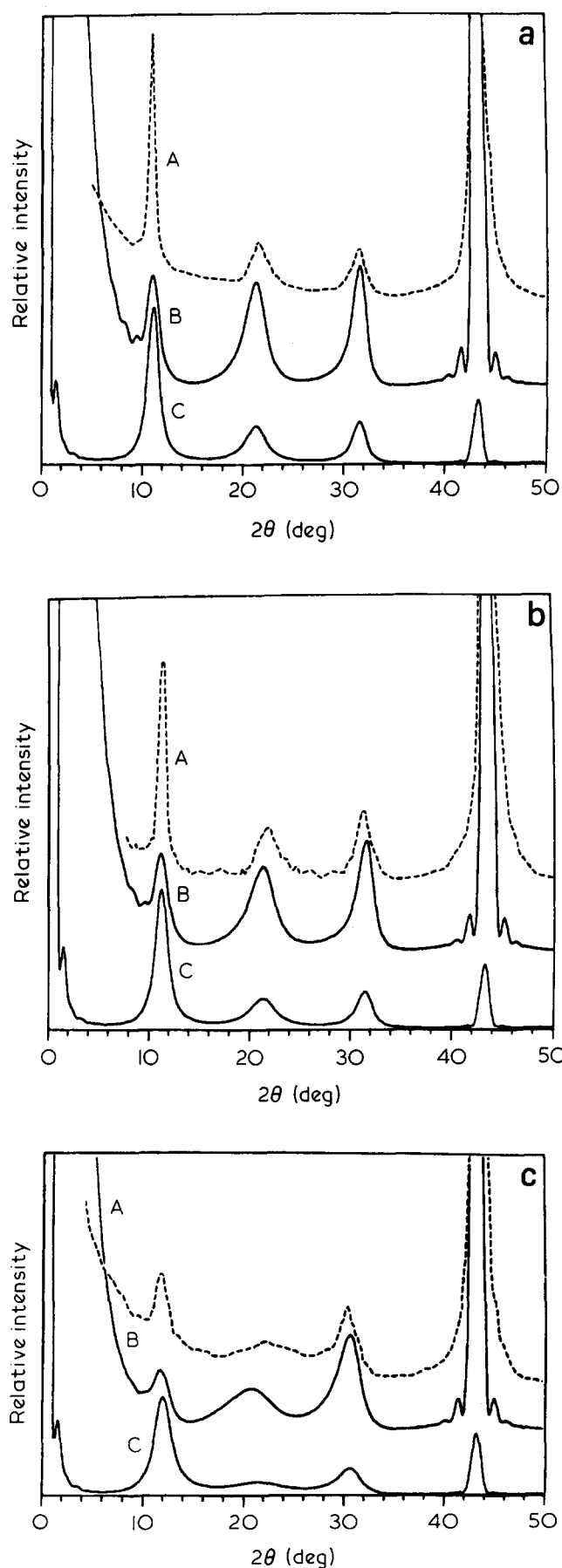


Table 2 Positions of observed meridional maxima

Composition, HBA/HNA	Experimental <i>d</i> -spacings from diffractometer (Å)	Calculated <i>d</i> -spacings from atomic model (Å)
25/75	8.11 ± 0.07	8.09
	4.15 ± 0.02	4.20
	2.85 ± 0.01	2.85
	2.09 ± 0.01	2.10
30/70	7.89	8.01
	4.09	4.21
	2.87	2.86
	2.09	2.10
50/50	7.49	7.61
	2.95	4.31
	2.95	2.95
	2.09	2.10
58/42	7.19	7.45
		4.40
	2.96	2.99
	2.08	2.11
75/25	6.70	7.04
	3.09	3.09
	2.09	2.11

Figure 3 Observed and calculated meridional intensity distributions of HBA/HNA copolyesters for five monomer ratios: (a) 25/75; (b) 30/70; (c) 50/50; (d) 58/42; (e) 75/25. The scans are as follows: A, observed intensity recorded on the diffractometer; B, theoretical intensity for the atomic model; C, theoretical intensity for the point model

at 7–8 Å is reduced in intensity while that at ~2 Å is enhanced. Electron diffraction of the homopolymer of HBA shows three meridionals at $d=6.3$ Å (weak), 3.15 Å (medium) and 2.1 Å (strong)⁶. The intensities match very well those predicted from the transform of the monomer. However, for all the copolymers, the first reflection is predicted weaker than observed, and this may be due to

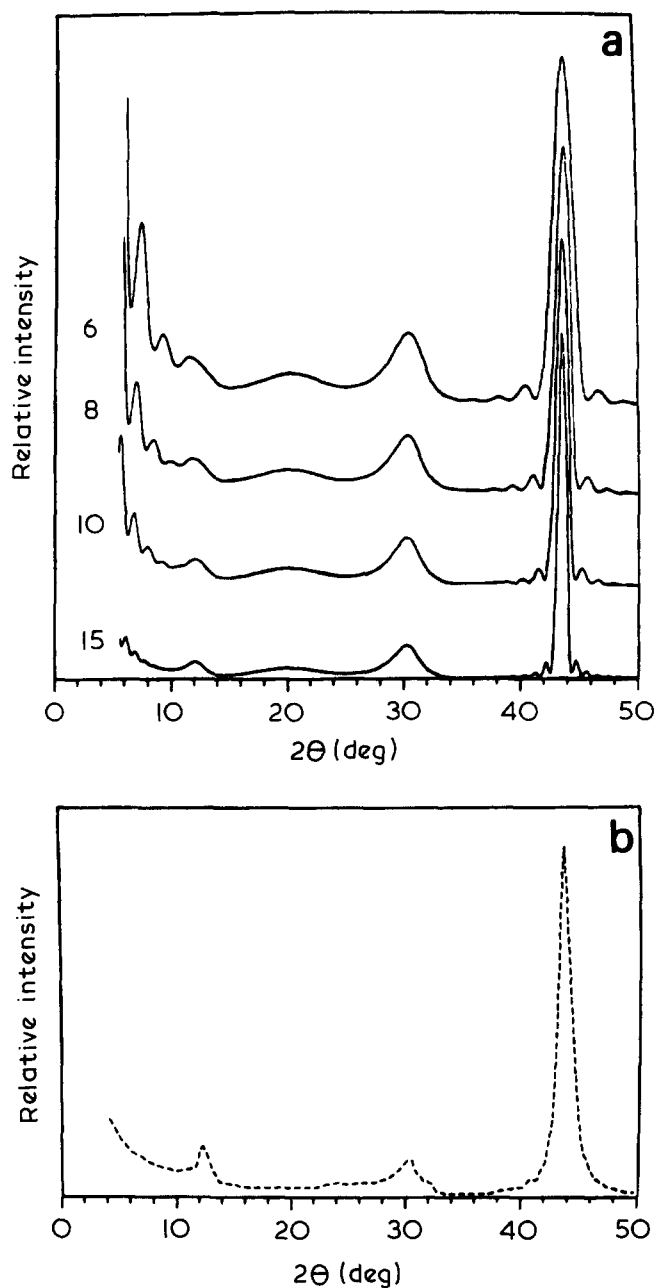


Figure 4 (a) Meridional intensity distributions for the 58/42 HBA/HNA copolymer calculated for (monodisperse) chain lengths of 6, 8, 10 and 15 monomers. (b) Observed intensity for the 58/42 copolymer on the same scale

the assumption that all monomers have the same conformation and lengths. As can be seen in *Figure 1b*, the ester oxygen-ester oxygen vector is not always parallel to the chain axis but rather is distributed in a range of $\pm 20^\circ$ about that axis. This arises from the non-linearity of the 2,6-naphthalene linkage, and is enhanced by the possibility of variable aromatic-carboxyl torsion angles. These effects can be expected to smooth the residue transforms to some extent and hence to increase the intensity in the region of the minimum at 6–8 Å.

So far we have not considered three-dimensional packing of the chains. The existence of sharp off-equatorial reflections is indicative of some three-dimensional order that could require a specific staggering of some chain sequences. Such a feature would be expected to modify the meridional intensity distribution from that calculated for a system with random axial

stagger, and may also explain the low intensity in the 7–8 Å region.

For the 50/50 and 58/42 compositions the predicted weak maximum at $d \approx 4.4$ Å is not seen in the diffractometer scans. However, some diffuse intensity is observed in this region, and very weak maxima are detected in the film data, but it is difficult to be sure whether these observations are truly axial intensity because of the arcing of the strong equatorial reflections.

$I(Z)$ in *Figure 3* has been calculated for an average chain length of 10 residues and, as has been stated, this corresponds to a persistence length rather than the degree of polymerization, which is thought to be in the range of 150. It can be seen in *Figure 4* that there is little effect on the shape of the transform once the chain length is increased beyond approximately eight residues, except that the peak at $d \approx 2.1$ Å gets progressively sharper. The latter can be regarded as a Bragg maximum because of the approximate 3:4 ratio of the lengths of HBA and HNA. The transforms for homopolymers of HBA and HNA have their third and fourth maxima, respectively, at $d \approx 2.1$ Å, and this interference is unaffected by copolymerization. Thus this peak gets sharper with increasing chain length and provides a method for estimating the axial persistence length. The data for the 58/42 monomer ratio show that the observed peak width is matched by (monodisperse) chain lengths of approximately 11 residues. Persistence length can be taken to mean the number of residues over which the stiff chain maintains the correlation of monomer lengths. The calculations are based on the assumption of constant monomer lengths: this can only be approximately correct because of inevit-

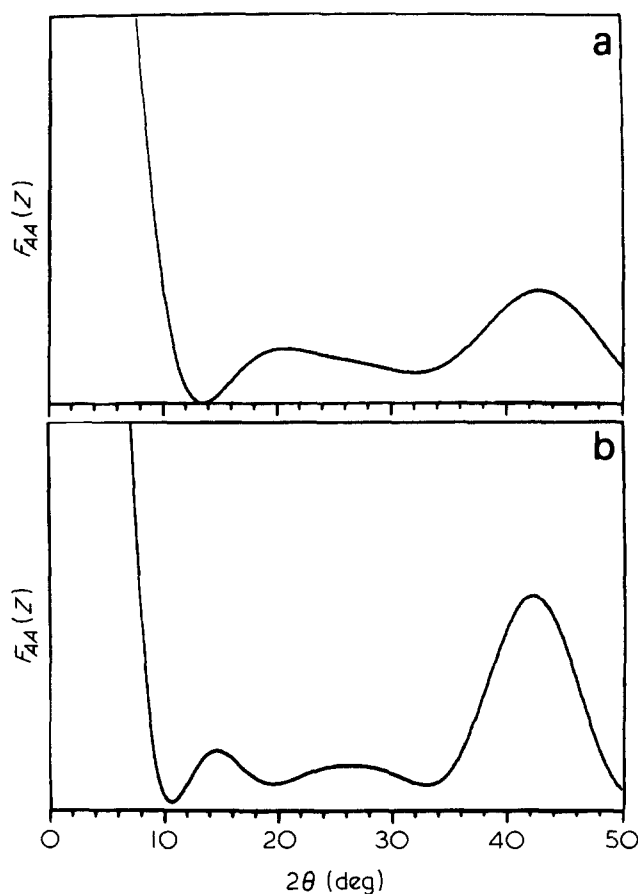


Figure 5 Fourier transforms of the monomer self-convolution functions, $F_{AA}(Z)$ for (a) HBA, and (b) HNA

able variations in residue orientations and torsion angles, and the calculations show that the approximation breaks down after ~ 11 residues. Nevertheless, the features in $Q(z)$ responsible for the maxima at $d > 2 \text{ \AA}$ are established by the time we reach these chain lengths.

The above predictions for the 2.1 \AA peak widths for the 58/42 copolymer are also obtained (approximately) for the other monomer ratios. However, the experimental data show an interesting trend in that the 2.1 \AA peak changes in width with the composition ratio, such that the persistence length increases from ~ 9 to ~ 13 as the HBA content increases. At this point it seems likely that the linearity of the chain will decrease progressively with increasing proportions of 2,6-naphthalene linkages, thereby reducing the persistence length. Further work is in progress on this aspect of the data.

CONCLUSIONS

Our previous work showed that a point residue approximation for a completely random chain of copoly(HBA/HNA) accurately predicted the positions of the observed meridional X-ray maxima. Extension of these calculations to an atomic model for the chains retains the match for the positions of the maxima and also gives good agreement between the observed and calculated intensities. The only discrepancy in the intensity agreement is for the maximum at $d = 7\text{--}8 \text{ \AA}$, which is generally predicted to be weaker than that observed. This is thought to arise from the assumption that all residues have the same conformation and axial orientation, and

the match can probably be improved by averaging over a range of residue orientations and torsion angles. The data contain information on the persistence length of the chain, which is a measure of the ordered conformation in the random copolymer. This is derived from the width of the Bragg maximum at $d \simeq 2.1 \text{ \AA}$, for which good agreement is obtained for models of the 58/42 copolymer with chain (persistence) lengths of 11 residues. Variation in the peak width with monomer ratio suggests that the persistence length increases with increasing HBA content.

ACKNOWLEDGEMENTS

We thank Dr J. B. Stamatoff of Celanese Research Company for the diffractometer data and for useful discussions. The work at Case Western Reserve University was supported by NSF Grant ISI81-16103, NSF Grant DMR81-07130 (from the Polymer Program), and from Celanese Research Company.

REFERENCES

- 1 Jin, J.-L., Antoun, S., Ober, C. and Lenz, R. S. *Br. Polym. J.* 1980, **12**, 132
- 2 Gutierrez, G. A., Chivers, R. A., Blackwell, J., Stamatoff, J. B. and Yoon, H. *Polymer* 1983, **24**, 937
- 3 Blackwell, J. and Gutierrez, G. A. *Polymer* 1982, **23**, 671
- 4 Blackwell, J., Gutierrez, G. A. and Chivers, R. A. *Macromolecules*, to be submitted
- 5 Calundann, G. W. (Celanese), US Patent 41 61 470, 1979
- 6 Blackwell, J., Lieser, G. and Gutierrez, G. A. *Macromolecules* 1983, **16**, 1418